

This is the accepted manuscript made available via CHORUS. The article has been published as:

Planar approximation for the frequencies of spin transfer oscillators

Ya. B. Bazaliy and F. Arammash

Phys. Rev. B **84**, 132404 — Published 5 October 2011

DOI: [10.1103/PhysRevB.84.132404](https://doi.org/10.1103/PhysRevB.84.132404)

Planar approximation for the frequencies of spin transfer oscillators

Ya. B. Bazaliy^{1,2,*} and F. Arammash³

¹*Department of Physics and Astronomy, University of South Carolina, Columbia, SC 29208*

²*Institute of Magnetism, National Academy of Science, Ukraine.*

³*Physics and Engineering Department, Benedict College, Columbia, SC 29204*

(Dated: September 12, 2011)

A large class of spin transfer oscillators use the free layer with a strong easy plane anisotropy, which forces its magnetization to move close to the plane. We show that in this situation the effective planar approximation provides a fast and accurate way of calculating the oscillator frequency.

PACS numbers: 75.76.+j, 75.78.-n, 85.75.-d

I. INTRODUCTION

Spin transfer devices exhibit regimes in which their magnetic moments perform perpetual precessional motions.^{1,2} In this case they are also called spin torque oscillators (STO). Magnetic oscillations induced by direct current are intensively studied experimentally³⁻¹¹ and theoretically.¹²⁻²² In the STO regime the energy is constantly supplied to the device from the current source through the spin transfer mechanism. At the same time it is lost through the usual dissipation mechanisms, accounted for by the Gilbert damping constant. In a state of steady precession the energy gain and loss are balanced on average. In the limit of small damping one observes the following general picture of STO operation.¹⁴ The magnetic moment moves close to the trajectory which it would follow in the absence of damping and spin transfer. The actual trajectory is a perturbation of the zero-damping trajectory, chosen so as to balance the small dissipation with the equally small energy gain. The main difficulty in describing the precession states is the lack of knowledge about the unperturbed trajectory which is a solution of the complicated non-linear Landau-Lifshitz-Gilbert (LLG) equation. Unless one considers a small radius precession near an equilibrium point, the analytic form of such a trajectory is usually unknown and one is forced to use numeric methods. In this paper we will consider a special class of spin transfer devices with dominating easy plane anisotropy. This anisotropy often arises from the thin disk shape of the magnetic layers found in the majority of experimental structures. Due to the dominating easy plane anisotropy the LLG equation can be approximated by an effective planar equation²³⁻²⁵ that is less complex and easier to treat analytically. Here we give a short derivation²⁶ of the planar approximation analytic expressions for the STO oscillation periods and compare them with the numeric results obtained without approximations.

II. MODEL

We will consider a macrospin description of a spin transfer device with one fixed and one free layer. The

moments of the fixed and free layers are given by unit vectors \mathbf{s} and \mathbf{n} with constant magnetization M_s . Magnetic dynamics of the free layer is governed by the LLG equation with a spin transfer term (see, e.g., Ref. 27)

$$\dot{\mathbf{n}} = \left[-\frac{\delta\varepsilon}{\delta\mathbf{n}} \times \mathbf{n} \right] + u[\mathbf{n} \times [\mathbf{s} \times \mathbf{n}]] + \alpha[\mathbf{n} \times \dot{\mathbf{n}}], \quad (1)$$

where the rescaled energy $\varepsilon = \gamma E/M_s$ is expressed through the total magnetic energy E of the free layer, γ is the (positive) gyromagnetic ratio, α is the Gilbert damping. The rescaled energy has dimensions of frequency and is directly related to the ferromagnetic resonance frequencies of the layer.

The spin-transfer magnitude u in the second term is given by

$$u = g(\vec{n}) \frac{\gamma(\hbar/2) I}{V M_s e}, \quad (2)$$

where V is the free layer volume, I is the electric current, and e is the electron charge. A frequently used approximation $g = \text{const}$ will be used for the efficiency factor. The rescaled current u has dimensions of frequency which facilitates its comparison with the anisotropy terms in LLG. Spin-transfer devices normally operate in the regime of $u \sim \alpha\varepsilon \ll \varepsilon$.

We assume the standard nanopillar anisotropy, i.e., an (x, y) easy plane with a constant K_p and an easy axis along x with a constant K_a . Magnetic field is applied along x as well. The rescaled energy function is

$$\varepsilon(\mathbf{n}) = \frac{\omega_p}{2} n_z^2 - \frac{\omega_a}{2} n_x^2 - h n_x,$$

where the new constants $\omega_p = \gamma K_p/M_s$, $\omega_a = \gamma K_a/M_s$, and $h = \gamma H$ have the dimensions of frequency. The fixed layer magnetization is assumed to be pointing along the easy axis, $\mathbf{s} = +\hat{x}$.

III. EFFECTIVE PLANAR DESCRIPTION

It was shown²⁴ that when the inequalities $\omega_p \gg \omega_a$ and $\omega_p \gg h$ hold, vector \mathbf{n} moves close to the easy plane and its magnetic dynamics can be described by an effective

planar equation governing the behavior of the in-plane (azimuthal) angle $\phi(t)$. The equation reads

$$\frac{\ddot{\phi}}{\omega_p} + \alpha_{eff}(\phi) \dot{\phi} = -\frac{d\varepsilon_{eff}}{d\phi}, \quad (3)$$

with effective energy and friction²⁴

$$\begin{aligned} \varepsilon_{eff} &= -\frac{\omega_a}{2} \cos^2 \phi - h \cos \phi, \\ \alpha_{eff} &= \alpha + \frac{2u \cos \phi}{\omega_p}. \end{aligned} \quad (4)$$

The analogy between Eq. (3) and the Newton equation of motion for a particle in a one-dimensional potential profile was employed in Ref. 24 to find the stabilization and destabilization currents of static and dynamic magnetic states in a nanopillar. Dynamic states correspond to the oscillations of the “effective particle” in the potential profile. They were treated analytically in the limit $\alpha \ll \sqrt{\omega_a/\omega_p}$ where the total energy $\varepsilon_{tot} = \dot{\phi}^2/2\omega_p + \varepsilon_{eff}$ of the particle is approximately conserved during one period of oscillations. In this case one can approximately express the fast-changing particle velocity as a function of its position and slow-changing $\varepsilon_{tot}(t)$

$$\dot{\phi}(t) \approx \pm \sqrt{2\omega_p(\varepsilon_{tot} - \varepsilon_{eff}(\phi))} = f(\phi, \varepsilon_{tot}). \quad (5)$$

During one period of oscillation T the total energy changes by a small amount

$$\Delta = -\int_0^T \alpha_{eff} \dot{\phi}^2 dt \ll \varepsilon_{tot}.$$

Using (5) one can express Δ and oscillations period as

$$\begin{aligned} \Delta &\approx -\oint \alpha_{eff}(\phi) f(\phi) d\phi, \\ T &= \int_0^T dt = \oint \frac{d\phi}{\dot{\phi}} \approx \oint \frac{d\phi}{f(\phi)}, \end{aligned} \quad (6)$$

where the integrals are taken along a closed trajectory corresponding to one period of frictionless motion. The total energy obeys an approximate equation

$$\frac{d\varepsilon_{tot}}{dt} \approx \frac{\Delta(\varepsilon_{tot})}{T(\varepsilon_{tot})}. \quad (7)$$

In the regime of persistent oscillations the total energy is constant, which implies $\Delta(\varepsilon_{tot}) = 0$. At a given u this equation determines the value of ε_{tot} and the endpoints of the integration contour in the first equation of the system (6). Knowing them, we can calculate T from the second equation in (6) and find the function $T(u)$. We perform the calculations for $u < 0$ which corresponds to the current-induced destabilization of the $\phi = 0$ equilibrium, or “parallel state”. Results for $u > 0$ can be then obtained using the symmetry of the switching diagram

with the respect to the simultaneous reflections $u \rightarrow -u$, $h \rightarrow -h$.

It was found²⁴ that persistent oscillations of the effective particle happen differently in the regimes of high $h > \omega_a$ and low $|h| < \omega_a$ fields. In the former case finite amplitude oscillations exist for $-u_2 < u < -u_1$ and full rotation motion is observed for $u < -u_2$. In the latter case finite amplitude oscillations exist for $-u_2 < u < -u_1$ and full rotation motion is observed for $u < -u_3$: There is a gap between the finite oscillations and full rotations regimes where there are no stable oscillating states.

At $h > \omega_a$, we find that the current and period of finite oscillations can be expressed through the oscillation amplitude ϕ_a as

$$u(\phi_a) = -\frac{\alpha\omega_p}{2} \frac{K_1(\phi_a)}{K_2(\phi_a)}, \quad (8)$$

$$T(\phi_a) = \frac{2K_3(\phi_a)}{\Omega}, \quad (9)$$

where $\Omega = \sqrt{\omega_a\omega_p}$ and

$$\begin{aligned} K_1(\phi_a) &= \int_{-\phi_a}^{\phi_a} \sqrt{R(\phi)} d\phi, \\ K_2(\phi_a) &= \int_{-\phi_a}^{\phi_a} \cos \phi \sqrt{R(\phi)} d\phi, \\ K_3(\phi_a) &= \int_{-\phi_a}^{\phi_a} \frac{d\phi}{\sqrt{R(\phi)}} \end{aligned}$$

$$R(\phi, \phi_a, h) = \cos^2 \phi - \cos^2 \phi_a + \frac{2h}{\omega_a} (\cos \phi - \cos \phi_a).$$

Using (8) and (9) one can draw a parametric plot of the function $T(u)$ by varying ϕ_a from zero to π .

The boundary between the finite oscillations and the full rotations is given²⁴ by the condition $\phi_a = \pi$

$$-u_2(h) = -\frac{\alpha\omega_p}{2} \frac{K_1(\pi, h)}{K_2(\pi, h)} \quad (h > \omega_a), \quad (10)$$

where we have explicitly indicated the dependence of the integrals on h . Note that (10) corrects formula (8) from Ref. 24 which is valid only for $h - \omega_a \ll \omega_a$.

For $u < -u_2$ the periods of full rotations are given by an analogous pair of equations

$$u(\delta) = -\frac{\alpha\omega_p}{2} \frac{L_1(\delta)}{L_2(\delta)} \quad (11)$$

$$T(\delta) = \frac{L_3(\delta)}{\Omega} \quad (12)$$

where $\delta = 2\omega_p(\varepsilon_{tot} - \varepsilon_{eff}(\pi))/\Omega > 0$ parameterizes the trajectories. With notation $\tilde{R} = R(\phi, \pi, h)$

$$\begin{aligned} L_1(\delta) &= \int_{-\pi}^{\pi} \sqrt{\tilde{R}(\phi) + \delta} d\phi, \\ L_2(\delta) &= \int_{-\pi}^{\pi} \cos \phi \sqrt{\tilde{R}(\phi) + \delta} d\phi, \\ L_3(\delta) &= \int_{-\pi}^{\pi} \frac{d\phi}{\sqrt{\tilde{R}(\phi) + \delta}}. \end{aligned}$$

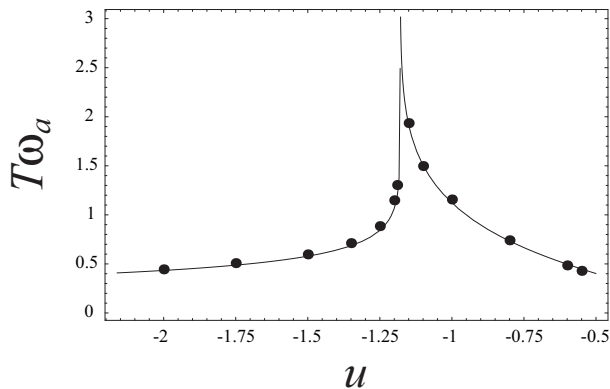


FIG. 1: Large field case. Comparison between the no-approximation numeric results (dots) and planar approximation expressions (lines) for the oscillations periods. Here $\omega_p = 100 \omega_a$, $h = 1.4 \omega_a$, $\alpha = 0.01$. The oscillation period diverges at $u = -u_2$

In the regime of small field, $|h| < \omega_a$ calculations for finite oscillations ($-u_2 < u < -u_1$) turn out to be identical with those performed in the previous section. Expressions (8) and (9) can be used to draw a parametric plot $T(u)$. The only difference is that now the oscillation amplitude ϕ_a changes from zero to the angle ϕ_m of the energy maximum, given by $\cos \phi_m = -h/\omega_a$.

For the currents exceeding the third threshold, $u < -u_3$, parametric expressions for current and period turn out to be identical to Eqs. (11) and (12), except that the meaning of \tilde{R} changes to $\tilde{R} = R(\phi, \phi_m, h) = (\cos \phi + h/\omega_a)^2$ in the definitions of the integrals $L_{1,2,3}$ and $\delta = 2\omega_p(\varepsilon(\phi) - \varepsilon(\phi_m))/\Omega > 0$.

Overall, equation pairs (8, 9) and (11, 12) give the planar approximation formulae for the periods of all spin transfer oscillations possible in our system. For the small amplitude oscillations regime with current just above the u_1 threshold the results (9) and (12) give the frequencies converging to $\sqrt{(\omega_a + h)\omega_p}$, i.e., to the Kittel's formula with a substitution $\omega_p + h \rightarrow \omega_p$ in accord with our approximation $h \ll \omega_p$. For other current values we will present the results of the theory as graphs (Figs. 1 and 2) for the periods $T(u, h)$ rather than for the frequencies since oscillations periods are more directly interpreted in terms of effective particle analogy.

IV. COMPARISON WITH THE NO-APPROXIMATION NUMERIC RESULTS

Oscillation periods can be found numerically by solving the LLG equation without approximations.

Fig. 1 compares the numeric LLG results with the planar approximation formula for the high field case, $h > \omega_a$. One observes a very good correspondence. Near the critical current $u = -u_2$ the periods of oscillations become infinite and their frequencies drop to zero.¹⁴ This is easy

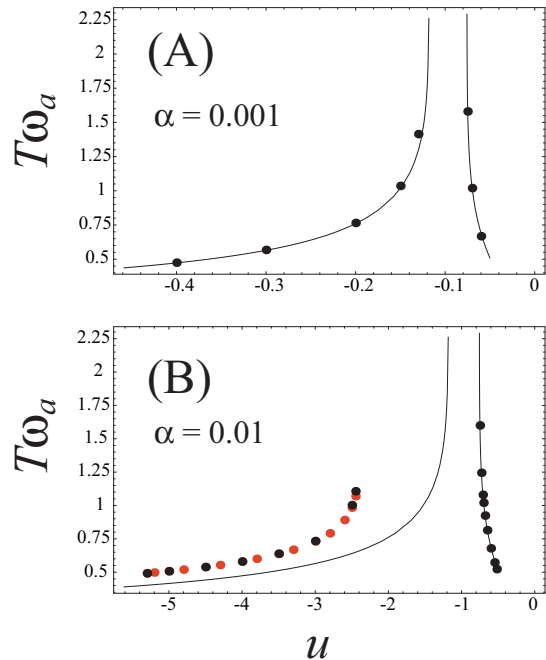


FIG. 2: (Color online) Small field case. Comparison between the no-approximation numeric results (dots) and planar approximation expressions (line) for the oscillations periods for $\omega_p = 100 \omega_a$, $h = 0.5 \omega_a$. The oscillation period diverges at $u = -u_2$ and $u = -u_3$ with no oscillations between the two thresholds. Top panel (A) gives results for $\alpha = 0.001$, where the agreement is very good. The bottom panel (B) shows a comparison for $\alpha = 0.01$. Planar approximation works well for finite precession, but the full rotations regime requires currents which are too large for the small friction approximation (11, 12) to be accurate. The exact solution of the planar equation (red (grey) dots) is still in very good agreement with the numeric solution of the LLG equation (black dots).

to understand from the effective particle analogy: at the critical current the particle travels between the two maxima of the energy profile that have the same height with the particle energy being equal to the potential energy at the maximum point. The motion near the maximum is infinitely slow and the period is infinite.

In the low field case, $0 < h < \omega_a$, the comparison of numeric and approximate results is shown in Fig. 2. In the top panel (Fig. 2A) the Gilbert damping is set to $\alpha = 0.001$, and the condition $|\alpha_{eff}| \ll \sqrt{\omega_a/\omega_p}$ is well satisfied for all current magnitudes on the graph. The correspondence between the numeric LLG results and the small damping approximation to the planar equation is very good. As expected, the oscillations period diverges at $u = -u_2$ and $u = -u_3$, with no oscillations between the two thresholds.

Fig. 2B shows results for $\alpha = 0.01$. We observe good correspondence between the LLG numeric results and our theory for finite oscillations, but the full rotations regime shows appreciable differences which become very large near the critical current. Their origin is the break-

down of the small damping approximation: for $\alpha = 0.01$ the currents in the full rotation regime are so large that the strong inequality $|\alpha_{eff}| \ll \sqrt{\omega_a/\omega_p}$ is not well satisfied. To prove that the small damping approximation is the source of the discrepancy we have solved the planar equation (3) numerically. The results (red (gray) dots in Fig. 2B) correspond very well to those obtained directly from LLG (black dots in Fig. 2B).

It is also instructive to compare the cases of large and small fields with the same value of Gilbert damping $\alpha = 0.01$ (Fig. 1 and Fig. 2B). One can see that the validity region of the small damping approximation extends at least to $u \approx -2$ in the case of large field. At the same time in the case of small fields this approximation is visibly violated for $u \approx -2$. The relative fragility of the small damping approximation in the full rotation regime in small fields can be traced to the presence of two energy maxima, $\phi = \pm\phi_m$, instead of just one maximum, $\phi = \pi$, in the large fields. The situation calls for more work on the approximate solutions of the effective planar equation (3) with variable damping.

V. CONCLUSIONS

We have shown that the planar approximation^{23,24} gives good results for the frequencies of spin transfer oscillators with dominating easy plane anisotropy. Analytic expressions for the oscillation periods were derived in the limit of small Gilbert damping. The mechanical analogy, associated with the effective planar equation, naturally explains the singular behavior of the precession frequency near the transition between in-plane and out-of-plane precessions.

A crucial advantage of the planar approximation is the resolution of the unperturbed trajectory problem. All one-dimensional trajectories are straight lines completely characterized by their endpoints. This simplification should help to develop theories of the large-angle precession regimes of planar spin torque oscillators in the presence of temperature fluctuations or other noise sources.

VI. ACKNOWLEDGEMENTS

This work was supported by the NSF grant DMR-0847159.

-
- * Electronic address: yar@physics.sc.edu
- ¹ J. Slonczewski, J. Magn. Magn. Mater. **159**, L1 (1996).
 - ² Ya. B. Bazaliy, B.A.Jones, and Shou-Cheng Zhang, J. Appl. Phys. **89**, 6793 (2001).
 - ³ M. Tsoi, A. G. M. Jansen, J. Bass, W.-C. Chiang, V. Tsoi, and P. Wyder, Nature **406**, 46 (2000).
 - ⁴ S. I. Kiselev, J. C. Sankey, I. N. Krivorotov, N. C. Emley, R. J. Schoelkopf, R. A. Buhrman, and D. C. Ralph, Nature, **425**, 380 (2003).
 - ⁵ W. H. Rippard, M. R. Pufall, S. Kaka, S. E. Russek, and T. J. Silva, Phys. Rev. Lett. **92**, 027201 (2004).
 - ⁶ J. C. Sankey, I. N. Krivorotov, S. I. Kiselev, P. M. Braganca, N. C. Emley, R. A. Buhrman, and D. C. Ralph, Phys. Rev. B **72**, 224427 (2005).
 - ⁷ W. H. Rippard, M. R. Pufall, and S. E. Russek, Phys. Rev. B **74**, 224409 (2006).
 - ⁸ D. Houssameddine, U. Ebels, B. Delat, B. Rodmacq, I. Firastrau, F. Ponthenier, M. Brunet, C. Thirion, J.-P. Michel, L. Prejbeanu-Buda, M.-C. Cyrille, O. Redon, B. Dieny, Nature Materials **6**, 447 (2007).
 - ⁹ O. Boulle, V. Cros, J. Grollier, L. G. Pereira, C. Deranlot, F. Petroff, G. Faini, J. Barnas, and A. Fert, Nature Physics **3**, 492 (2007) .
 - ¹⁰ T. Devolder, A. Meftah, K. Ito, J. A. Katine, P. Crozat, and C. Chappert, J. Appl. Phys., **101**, 063916 (2007).
 - ¹¹ D. Houssameddine, U. Ebels, B. Dieny, K. Garello, J.-P. Michel, B. Delaet, B. Viala, M.-C. Cyrille, J. A. Katine, and D. Mauri, Phys. Rev. Lett. **102**, 257202 (2009).
 - ¹² A. D. Kent, B. Ozyilmaz, and E. del Barco, Appl. Phys. Lett. **84**, 3897 (2004).
 - ¹³ S. M. Rezende, F. M. de Aguiar, and A. Azevedo, Phys. Rev. Lett. **94**, 037202 (2005).
 - ¹⁴ G. Bertotti, C. Serpico, I. D. Mayergoyz, A. Magni, M. d'Aquino, and R. Bonin, Phys. Rev. Lett. **94**, 127206 (2005).
 - ¹⁵ C. Serpico, M. d'Aquino, G. Bertotti, and I. D. Mayergoyz, J. Magn. Magn. Mat. **290-291**, 502 (2005).
 - ¹⁶ C. Serpico, J. Magn. Magn. Mat. **290-291**, 48 (2005).
 - ¹⁷ R. Bonin, C. Serpico, G. Bertotti, I. D. Mayergoyz and M. d'Aquino, Eur. Phys. J. B **59**, 435 (2007).
 - ¹⁸ X. Wang, G. E. W. Bauer, and A. Hoffmann, Phys. Rev. B, **73**, 054436 (2006).
 - ¹⁹ J.-V. Kim, V. Tiberkevich, and A. N. Slavin, Phys. Rev. Lett. **100**, 017207 (2008).
 - ²⁰ V. S. Tiberkevich, A. N. Slavin, and J.-V. Kim, Phys. Rev. B **78**, 092401 (2008).
 - ²¹ J.-V. Kim, Q. Mistral, C. Chappert, V. S. Tiberkevich, and A. N. Slavin, Phys. Rev. Lett. **100**, 167201 (2008).
 - ²² A. Slavin and V. Tiberkevich, IEEE Trans. Magn. **44**, 1916 (2008).
 - ²³ Ya. B. Bazaliy, Appl. Phys. Lett. **91**, 262510, (2007).
 - ²⁴ Ya. B. Bazaliy, Phys. Rev. B **76**, 140402(R), (2007).
 - ²⁵ Ya. B. Bazaliy, Proceedings of SPIE Conference, Spintronics II, 7398, 73980P-1 (2009).
 - ²⁶ For a more detailed discussion see arXiv:1109.1335 (2011).
 - ²⁷ Ya. B. Bazaliy, B. A. Jones, and Shou-Cheng Zhang, Phys. Rev. B, **69**, 094421 (2004).